Chinese Chemical Letters 32 (2021) 3522–3525

Contents lists available at ScienceDirect

Chinese Chemical Letters

journal homepage: www.elsevier.com/locate/cclet

Communication

Tunable organic particles: An efficient approach from solvent-dependent Schiff base macrocycles

Ying Xiong[a,b], Chao Huang[a], Hongjuan Liu[a], Rui Yi[a], Bi-Xue Zhu[a,*], Xin-Long Ni[a,c,*]

[a] Key Laboratory of Macrocyclic and Supramolecular Chemistry of Guizhou Province, Guizhou University, Guiyang 550025, China
[b] School of Chemistry and Materials, Guizhou Normal University, Guiyang 550025, China
[c] College of Chemistry and Chemical Engineering, Key Laboratory of the Assembly and Application of Organic Functional Molecules of Hunan Province, Hunan Normal University, Changsha 410081, China

ARTICLE INFO

Article history:
Received 2 March 2021
Revised 28 April 2021
Accepted 30 April 2021
Available online 8 May 2021

Keywords:
Schiff base
Organic particles
Macrocycle
Noncovalent interaction
Self-assembly

ABSTRACT

The synthesis of cyclopolymers upon controlling the degree of macrocyclic polymerization, followed by the discovery of new properties has attracted increasing attention in supramolecular chemistry. Herein, a Schiff-base condensation method performed at room temperature was used to control the formation of [1 + 1] and [2 + 2] macrocycles. In pure MeOH, the isomer [1 + 1] macrocycles were synthesized and organic particles such as dendritic, rods, and solid microspheres were directly precipitated from the reaction solution. The [1 + 1] macrocycles can be efficiently converted into their corresponding [2 + 2] macrocycles accompanied by the tunable morphology of the organic particles when *n*-hexane was added to the MeOH solution. Further studies showed that these organic particles have potential application toward the selective removal of Cd^{2+} ions with different adsorption ability in MeOH solution.

Organic particles, have attracted a large amount of attention in materials science because of their tunable structures, facile fictionalization, and tailorable fashions with flexible particle parameters, including shape, size, and surface morphology [1,2]. As a result, organic particles exhibit unique advantage in applications such as catalysis [3,4], sensing [5,6], photoelectrical devices [7,8], and biomedical theranostics [9–13]. Due to the properties of organic particles being heavily dependent on their morphological parameters, the controlled formulation of organic particles has become a key topic in this research field. Nanoprecipitation [14], emulsion [15], and self-assembly [16] are the most widely used methods for the fabrication of organic particles.

Despite extensive investigations on the post-synthesis self-assembly of organic molecules and macrocycle-based host-guest systems, few studies have demonstrated the ability to control both the molecular structure and morphology of the self-assembly-derived particles in one step. Recently, our studies have suggested that organic particles can be directly precipitated in a Schiff-base cyclization reaction with tunable chemical and morphology structures from the same starting materials by simply adjusting the reaction solvent [17,18]. For example, solid microspheres were formed in pure MeOH by yielding [2 + 2] Schiff base macrocycles and numerous nano-vesicles with uniform size were produced in a mixed solution of MeOH/H_2O (v/v ≤ 1:2), which was attributed to the reaction being completely switched to favor the formation of [1 + 1] Schiff base macrocycles. However, when the solvent was changed to a mixture of MeOH/H_2O (v/v ≥ 1:2), the reaction between the organic precursors yielded both [2 + 2] and [1 + 1] macrocycles, forming core−shell-shaped spherical nanoparticles with a [2 + 2] macrocycle as the core and [1 + 1] macrocycle as the shell *via* narcissistic self-sorting [18]. Evidently, our studies indicate that the skeleton of the Schiff base macrocycles and their resulting inter-and intramolecular dynamic and reversible non-covalent interactions are the key factors for the formation of the organic particles.

With these observations in mind, we continue our interest in the design and synthesis of solvent dependent Schiff base macrocycles for organic particles.

In particular, we want to know what will happen to the particle morphology upon subtle modification of the skeleton of the Schiff base macrocycle. As shown in Scheme 1 and Supporting information, a Schiff-base condensation method at room temperature was used to form [1 + 1] macrocycles (**M_1**, **M_2**, and **M_3**) and [2 + 2] macrocycles (**M_4** and **M_5**), in which the 2,6-diimide pyridine core derived *ortho*-, *meta*- and *para*-diamines (**A_1**, **A_2**, **A_3**) and pyrrole-based dialdehyde (**B_1**) were used as the reaction precursors, respectively. In pure MeOH, [1 + 1] macrocycles were synthesized,

* Corresponding authors.
E-mail addresses: bxzhu@gzu.edu.cn (B.-X. Zhu), longni333@163.com (X.-L. Ni).

https://doi.org/10.1016/j.cclet.2021.04.060
1001-8417/

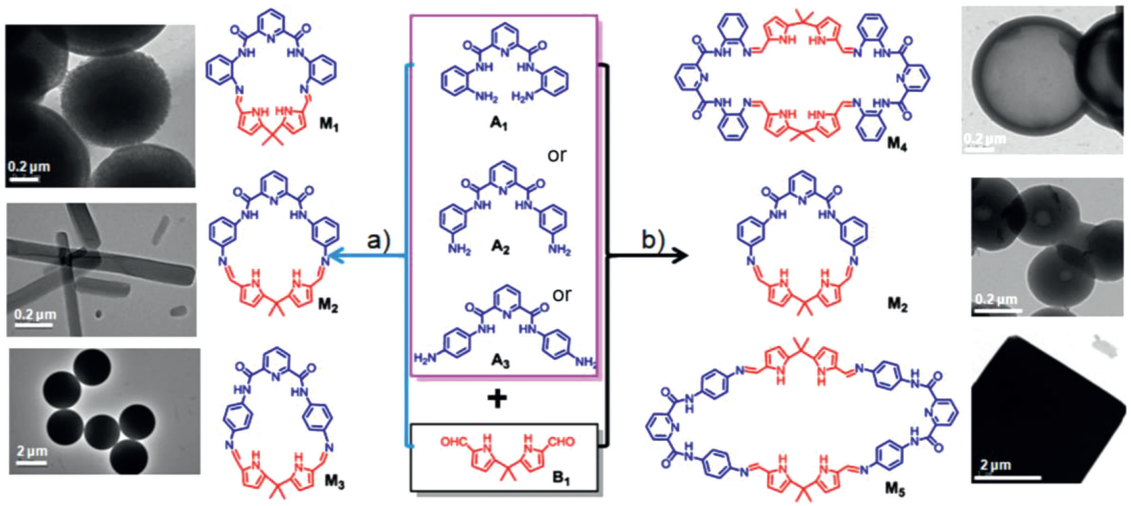

Scheme 1. (a) The chemical structures of $\mathbf{M_1}$, $\mathbf{M_2}$, and $\mathbf{M_3}$ and their corresponding TEM images recorded in CH_3OH. (b) The chemical structures of $\mathbf{M_4}$, $\mathbf{M_2}$ and $\mathbf{M_5}$ and their corresponding TEM images recorded in CH_3OH/*n*-hexane (1:5, v/v).

whereas organic particles such as dendritic, rods, and solid microspheres were formed from the assembly of $\mathbf{M_1}$, $\mathbf{M_2}$ and $\mathbf{M_3}$, respectively, which is very different from our previously reported results. The conversion from one macrocycle to another cannot be efficiently carried out by the addition of water to the MeOH solution. However, [1 + 1] macrocycles can be fully converted to their corresponding [2 + 2] macrocycles accompanied by a change in the morphology of the particles when *n*-hexane was added to the MeOH solution, except for the *meta*-substituted diamine, where the [1 + 1] macrocycle was maintained, while the particles changed from rods to solid microspheres. Further studies suggested that the organic particles have potential application toward the selective binding of Cd^{2+} ions. The results indicated that slight changes in both the macrocycle structure and solvent can be used to switch the morphologies of the organic particles.

Scanning electron microscopy (SEM) and transmission electron microscopy (TEM) images suggest that the precipitates of $\mathbf{M_1}$ were composed of numerous dendritic-like nanoparticles (Scheme 1 and Fig. 1a), while the assembly of $\mathbf{M_2}$ formed a rod-like morphology (Fig. 1d) with approximate diameters in the range of 200–400 nm and lengths of several micrometers. Micro-solid spheres with remarkably uniform diameters (3 μm) were observed in the precipitate formed from $\mathbf{M_3}$ (Fig. 1g). Interestingly, when water was added to the CH_3OH reaction mixture according to our previous experimental procedure, we found that only some of the [1 + 1] macrocycles of $\mathbf{M_1}$ and $\mathbf{M_3}$ were converted into their corresponding [2 + 2] macrocycles (Fig. S2 in Supporting information), but the corresponding particle morphologies were changed (Fig. S3 in Supporting information). For example, a mixture of micro-spheres and solid spheres were observed in the *ortho*-Schiff base macrocycles and a mixture particle of grid and solid spheres were observed in the *para*-Schiff base macrocycles. Unexpectedly, the *meta*-Schiff base [1 + 1] macrocycle of $\mathbf{M_2}$ was stability exists in the presence of water, but the morphology of the particles was completely transferred from rods to micro-solid spheres.

Obviously, the present experimental results are very different to our previous studies [18]. In that case, [2 + 2] Schiff base macrocycles with solid microspheres were formed in CH_3OH and [1 + 1] Schiff base macrocycles with a nano-vesicle morphology were formed when water was added to the CH_3OH solution up to 2:1 (v/v). From a structural viewpoint, the largest difference was an O atom instead of the NH moiety in the present macrocycles. We proposed that the different hydrogen binding ability between the

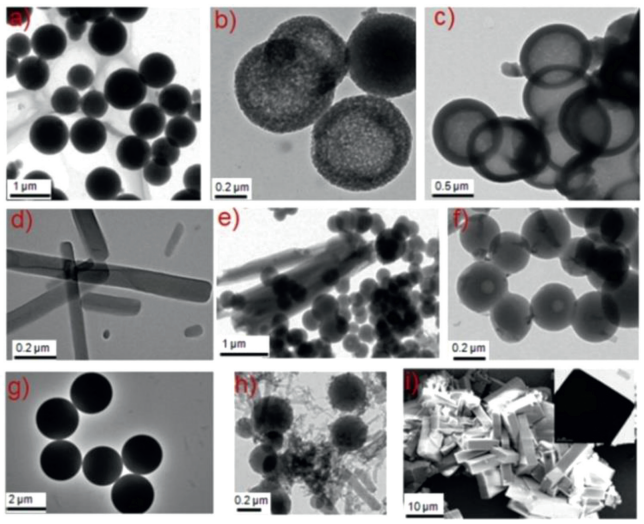

Fig. 1. TEM images of the precipitates of Schiff base macrocycles formed in CH_3OH (20 mL) containing different amounts of *n*-hexane: (a-c) $\mathbf{A_1}$ reaction with $\mathbf{B_1}$ in CH_3OH, CH_3OH/*n*-hexane (1:1, v/v), and CH_3OH/*n*-hexane (1:5, v/v), respectively; (d-f) $\mathbf{A_2}$ reaction with $\mathbf{B_1}$ in CH_3OH, CH_3OH/*n*-hexane (1:1, v/v), and CH_3OH/*n*-hexane (1:5, v/v), respectively; (g-h) $\mathbf{A_3}$ reaction with $\mathbf{B_1}$ in CH_3OH and CH_3OH/*n*-hexane (1:1, v/v); (i) SEM and TEM (insert) images of $\mathbf{A_3}$ reaction with $\mathbf{B_1}$ in CH_3OH/*n*-hexane (1:5, v/v).

NH and O atoms was the key factor resulting in the different degrees of macrocycle polymerization and self-assembly induced organic particles. After studying many other solvents, we found that using *n*-hexane, a classical non-polar solvent, as a co-solvent in the CH_3OH solution can drive the formation of the *ortho*- and *para*-derived [2 + 2] Schiff base macrocycles ($\mathbf{M_4}$ and $\mathbf{M_5}$).

When different volumes of *n*-hexane were added to the CH_3OH solution, the Schiff base reaction was performed in an identical manner to the [1 + 1] cycloreaction at room temperature for 3 h. The ^1H NMR and MS results suggested that *ortho*- and *para*-appended [2 + 2] macrocycles ($\mathbf{M_4}$ and $\mathbf{M_5}$) were solely formed when >100 mL of *n*-hexane was added to the CH_3OH solution (20 mL) (Fig. S4 in Supporting informaiton). The SEM and TEM images revealed that the corresponding particle morphology was switched to nanovesicles (Fig. 1c) in $\mathbf{M_4}$ and block-shaped sheets with micrometer dimensions in $\mathbf{M_5}$ (Fig. 1i), respectively. Interestingly, in-

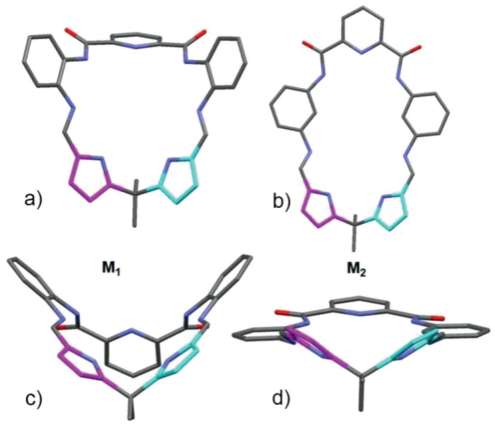

Fig. 2. Top- and side-view of the X-ray structure of $\mathbf{M_1}$ (a, c) and $\mathbf{M_2}$ (b, d).

termediate morphologies of the macrocycle structure dependent particles were also obtained in the case of MeOH/*n*-hexane (> 1:5, v/v). For example, a loosely core-shell morphology (Fig. 1b) and a mixture of nanosheets and solid spheres (Fig. 1e) were formed in the reaction of $\mathbf{A_1}$ and $\mathbf{A_3}$ with $\mathbf{B_1}$ in a mixed solution of CH_3OH/*n*-hexane (v/v = 1:1), respectively. The ^1H NMR and MS results indicate that the particles were composed of $\mathbf{M_1}$ and $\mathbf{M_4}$, and $\mathbf{M_3}$ and $\mathbf{M_5}$, respectively (Fig. S5 in Supporting information). In addition, the experiment results suggest that the molecular structure of $\mathbf{M_2}$ was still retained in the presence of *n*-hexane, but the particle morphology was changed from rods to solid nanospheres in the mixed solvent, which may be attributed the different hydrogen bonding interactions of $\mathbf{M_2}$ in the mixed CH_3OH/*n*-hexane solution [19]. This result implied that the non-covalent interactions in these macrocycles also play an important role in fabricating of the organic particles.

Single-crystal X-ray diffraction revealed that $\mathbf{M_1}$ has a [1 + 1]-condensation and adopts a highly bent saddle-shaped structure (Figs. 2a and c). Furthermore, it should be noted that the benzene ring and pyrrole ring located on the same side chain of the saddle-shaped structure was almost coplanar; this molecular configuration provides an ideal scaffold for intermolecular CH–π interactions. As indicated in Fig. 3a, each macrocyclic molecule ($\mathbf{M_1}$) was alternately linked in an opposite orientation *via* intermolecular CH–π interactions. Namely, $\mathbf{M_1}$ was arranged in an alternate "front–behind–front–behind" fashion to stack with each other from cavity to cavity to form a figure eight-shaped 1D columnar structure viewed along a-axis (Fig. 3b). Careful analysis of the packing revealed that the two pyrrole C–H bonds (C16 and C22), as well as the bridging methylene proton (C19H) in $\mathbf{M_1}$ take part in the CH–π interaction with its adjacent molecules. Furthermore, the 1D columnar structures were produced into two- and three-dimensional networks *via* intermolecular CH–π interactions between the pyrrole protons (C15H or C23H) and aryl rings in $\mathbf{M_1}$ located in the adjacent columns (Fig. 3f). A noteworthy point is that all of the $\mathbf{M_1}$ molecules are assembled by intermolecular non-covalent CH–π interactions.

In contrast, the X-ray crystal structure of macrocycle $\mathbf{M_2}$ revealed that it has a flat oval cavity (Fig. 2b). As indicated in Fig. 3c, the $\mathbf{M_2}$ molecules were linked alternately in an alternate "up–down–up–down" fashion to form intermolecular offset face-to-face π-stacking interactions between the coplanar aryl moieties *via* sliding of the adjacent $\mathbf{M_2}$ molecules. Careful analysis of the packing revealed that the driving force for the directional 1D aggregation is the π-stacking interactions with the coplanar aryl rings moieties in $\mathbf{M_2}$, and the distances between the aryl-ring centers for

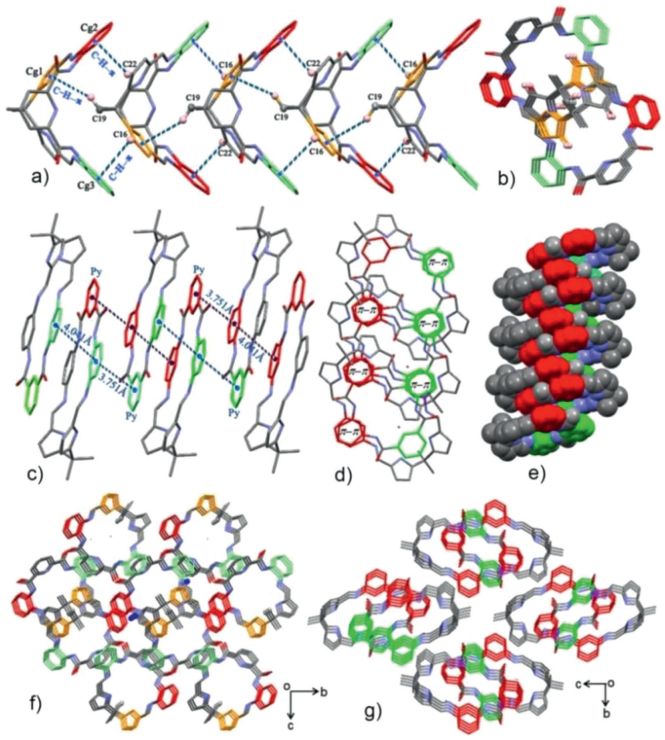

Fig. 3. (a) Side- and (b, f) top-view of the CH-π interaction directed self-assembly of $\mathbf{M_1}$ and (c, e) side- and (d, g) top-view of the π-π interaction directed self-assembly of $\mathbf{M_2}$ in the solid-state.

the π interactions were 3.75 and 4.04 Å, respectively, and provide strong pillars for the 1D columnar structure (Figs. 3d-g).

The X-ray structure of the *para*-derived [2 + 2] Schiff base macrocycle ($\mathbf{M_5}$) indicates that a large cavity (20.16 Å × 18.21 Å) was constructed (Fig. S6 in Supporting information), in which each side of the two pyrrole rings were almost twisted by 180° to link the bis(2-aminophenyl)pyridine-2,6-dicarbonyl amide moieties *via* imine bonds (Fig. S6b). Interestingly, it was notable that only one benzene ring was coplanar with one of the central pyridine moieties in $\mathbf{M_5}$ (marked with red and green color in Fig. S6a). Closer inspection suggested that the $\mathbf{M_5}$ molecules were also linked alternately in an "up–down–up–down" fashion like $\mathbf{M_2}$ *via* π-π stacking interactions formed between the coplanar aromatic moieties of the adjacent $\mathbf{M_5}$ molecules (Fig. S6d). However, different from the 1D columnar assembly of $\mathbf{M_2}$ formed *via* π-π interactions, the assembly of $\mathbf{M_5}$ directed by the π-π stacking interactions led to 2D columnar structures (Fig. S6c) and then further formed 3D networks (Fig. S6e) *via* intermolecular CH–π interactions formed between the methylene protons and pyrrole rings in the adjacent $\mathbf{M_5}$ molecules (Fig. S7 in Supporting information).

Accordingly, the X-ray structures of $\mathbf{M_1}$, $\mathbf{M_2}$ and $\mathbf{M_5}$ indicate that the subtle modification of the skeleton of the Schiff base macrocycles can generate different non-covalent interactions and assembly of the macrocycles in the solid-state, which should be a key factor leading to the various morphologies of their corresponding macrocycles-based organic particles.

Our recent studies suggest that the twisted Schiff base macrocycle derived micro-/nanospheres has potential application as a nanocarrier for Fe^{3+} [20]. This may be attributed to the different macrocyclic structure and metal coordinating atoms (N^N) to those previously reported. We found that the present work obtained macrocycles-based organic particles exhibiting adsorption ability for Cd^{2+}. Upon addition of these solid organic particles (each of 1.0 mg/mL) into the CH_3OH solution, which was a mixture solution

of Zn^{2+}, Cd^{2+}, Pb^{2+}, Hg^{2+}, Ni^{2+}, Fe^{3+}, Cu^{2+}, Co^{2+}, Cr^{3+} ions (each of 100.0 μmol/L), respectively. As show in Fig. S8 (Supporting information), elemental mapping analysis of the energy-dispersive X-ray spectroscopy (EDS) results showed that only Cd^{2+} was found in the spectra. It was found that Cd^{2+} ions were uniformly distributed on the $\mathbf{M_1}$ derived nanoparticles and less Cd^{2+} ions were adsorbed in the $\mathbf{M_2}$, and $\mathbf{M_3}$ derived particles. In particular, there is no clear Cd^{2+} adsorption distribution in the $\mathbf{M_2}$-based rod-like morphology (Figs. S8b, S9 and Table S1 in Supporting information). UV-vis absorption experiment results indicated that 2:1 complex of macrocycles with Cd^{2+} were formed in solution (Fig. S10 in Supporting information). In addition, it was found that $\mathbf{M_4}$ and $\mathbf{M_5}$ have no adsorption of Cd^{2+}. Evidently, these results suggested that the Schiff-base macrocycle based organic particles has selective removal ability of Cd^{2+} ions from the solution. Meanwhile, these results also revealed that the metal ion adsorption ability of the Schiff base macrocycles was not only dependent on their molecular structures, but is also dependent on the self-assembly induced morphologies of organic particles.

In summary, we have further developed an insight into the controlled synthesis of Schiff base macrocycles and their corresponding organic particles. X-ray structure analysis revealed that unusual non-covalent interactions, such as CH-π and π-π stacking, play key roles in directing the assembly of the macrocycles into organic particles. Considering that a lot of attention has been focused toward controlling the synthesis of macrocycles and exploiting their new properties in supramolecular chemistry, the present work may provide a new understanding of macrocyclic molecular structure design, micro-/nano-organic particle fabrication, and their potential applications.

Declaration of competing interest

There are no conflicts to declare.

Acknowledgments

This work was supported by the National Natural Science Foundation of China (Nos. 21961007 and 21871063), the Science and Technology Foundation of Hunan Province (No. 2020JJ2021).

Supplementary materials

Supplementary material associated with this article can be found, in the online version, at doi:10.1016/j.cclet.2021.04.060.

References

[1] D. Horn, J. Rieger, Angew. Chem. Int. Ed. 40 (2001) 4330–4361.
[2] S. Wagner, A. Gondikas, E. Neubauer, T. Hofmann, F. Kammer, Angew. Chem. Int. Ed. 53 (2014) 12398–12419.
[3] J.F. Chen, E.S. Garcia, S.C. Zimmerman, Acc. Chem. Res. 53 (2020) 1244–1256.
[4] J.M. Zhou, X.F. Zhu, Q.Y. Cheng, et al., Inorg. Chem. 59 (2020) 9177–9187.
[5] D. Ding, K. Li, B. Liu, B.Z. Tang, Acc. Chem. Res. 46 (2013) 2441–2453.
[6] J. Qian, B.Z. Tang, Chem 3 (2017) 56–91.
[7] Y.L. Yan, Y.S. Zhao, Chem. Soc. Rev. 43 (2014) 4325–4340.
[8] K.S. Daskalakis, A.I. Väkeväinen, J.P. Martikainen, T.K. Hakala, P. Törmä, Nano Lett. 18 (2018) 2658–2665.
[9] K. Li, B. Liu, Chem. Soc. Rev. 43 (2014) 6570–6597.
[10] M. Overchuk, G. Zheng, Biomaterials 156 (2018) 217–237.
[11] X. Fu, L. Hosta-Rigau, R. Chandrawati, J.W. Cui, Chem 4 (2018) 2084-2107.
[12] Z. Wang, B. Guo, E. Middha, et al., ACS Appl. Mater. Interfaces 11 (2019) 11167–11176.
[13] L. Huang, Z.J. Li, Y. Zhao, et al., J. Am. Chem. Soc. 138 (2016) 14586–14591.
[14] D.F. Liu, S. Cito, Y.Z. Zhang, et al., Adv. Mater. 27 (2015) 2298–2304.
[15] J.P. Rao, K.E Geckeler, Prog. Polym. Sci. 36 (2011) 887–913.
[16] [a] G.C. Yu, K.C. Jie, F.H. Huang, Chem. Rev. 115 (2015) 7240–7303.
[b] T. Xiao, L. Zhou, X.Q. Sun, et al., Chin. Chem. Lett. 31 (2020) 1–9.
[c] S. Li, Y. Gao, Y. Ding, A. Xu, H. Tan, Chin. Chem. Lett. 32 (2021) 313–318.
[d] Y. Hou, S. Li, Z. Zhang, L. Chen, M. Zhang, Polym. Chem. 11 (2020) 254–258.
[17] H.Y. Chen, C. Huang, Y.Z. Ding, et al., Chem. Sci. 10 (2019) 490–496.
[18] H.Y. Chen, C. Huang, Y.X. Deng, et al., ACS Nano 13 (2019) 2840–2848.
[19] L.S. Shimizu, S.R. Salpage, A.A. Korous, Acc. Chem. Res. 47 (2014) 2116–2127.
[20] Q. Yu, X.D. Zhang, S.T. Wu, et al., Chem. Commun. 56 (2020) 2304–2307.